Effects of Connection Stiffness and Plasticity on the Service Load Behavior of Unbraced Steel Frames

M. ASGHAR BHATTI and JAMES D. HINGTGEN

ABSTRACT

Accurate determination of the relative restraint of beam-to-column connections is important for both the strength and serviceability of structural frames. Overestimating the connection restraint can result in underestimating lateral sway and underestimating the connection restraint can lead to underestimating forces developed in the beams and columns. Both conditions can influence structural instability. This paper examines the effects that certain connection parameters have on the serviceability limit state of unbraced steel frames. The connections are modeled as elastic-perfectly plastic and are described by their elastic stiffness and the ultimate moment capacity. The second order *P*-delta effects are included. The effect of connection geometry on lateral sway for an unbraced, 3-bay and 5-story office building is studied. Three types of bolted connections: single and double web-angle, top- and seat-angle, and top- and seat-angle with double web-angles are examined and their effect on lateral sway is compared with and without second order *P*-delta effects.

1. INTRODUCTION

In conventional frame analysis the beam-to-column connections are idealized either as pinned connections which resist no moment or as rigid connections which assume no relative change in joint angle. Most real connections fall in between these two extremes. Every joint will deform to some extent and will resist a certain amount of bending moment. The relationship between beam end moment, M, and the relative change in angle, θ_r, can be described with the use of a moment-rotation diagram. Figure 1 is an example of a typical moment-rotation diagram for a bolted connection.[1]

Accurate determination of the relative restraint of beam-to-column connection is important for both the strength and serviceability of structural frames. Overestimating the connection restraint can result in underestimating lateral sway and underestimating the connection restraint can lead to underestimating forces developed in the beams and columns. Both conditions can influence structural instability.

In order to provide for a realistic recognition of the actual degree of connection restraint, Chapter A of the AISC *Manual of Steel Construction: Load and Resistance Factor Design* (LRFD),[2] specifies two types of construction: Fully restrained beam-to-column connections (FR) and partially restrained beam-to-column connections (PR). FR construction is the traditional method of analyzing frames where it is assumed that no relative rotation occurs between the beam and column. Whereas, in PR construction it is assumed that there is "evidence of a predictable portion of full end restraint."[2] Extensive research has been done to gather this "evidence" and considerable data is available from tests of connections.[3] However, for the majority of designers, design and analysis of frames with PR construction still seems impractical when compared to relative simplicity of traditional FR construction.

In order to develop a feel for PR frame analysis a detailed parametric study is carried out using a computer program developed by the authors, called FlexFrame.[4] The program includes second order *P*-delta effects and flexibly connected joints. Effect of connection geometry on frame sway and stability for a typical, unbraced, 3-bay and 5-story office building is studied. The analysis is done using three types of bolted connections: single and double web-angle, top- and seat-angle, and top- and seat-angle with double web-angles. The connections are modeled as elastic-perfectly plastic and are described by the parameters K_i, the elastic stiffness, and

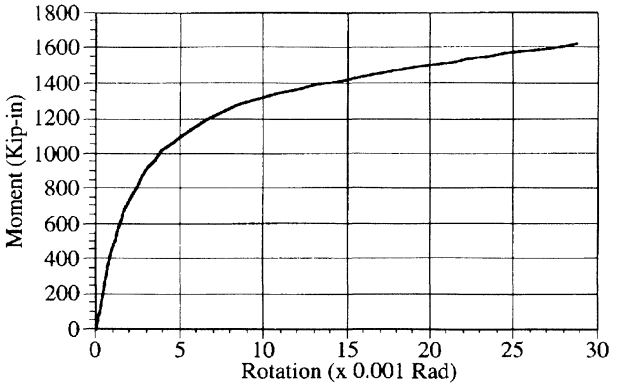

Fig. 1. Typical moment-rotation diagram.

M. Asghar Bhatti is associate professor, department of civil and environmental engineering, University of Iowa, Iowa City, IA.

James D. Hingtgen is graduate student, department of civil and environmental engineering, University of Iowa, Iowa City, IA.

M_u the ultimate moment capacity, as shown in Figure 2. These parameters are determined from equations which were formulated using finite element analysis by Kishi and Chen.[5]

Section 2 presents a summary of different moment-rotation models for joints in steel frames. Section 3 outlines the basic frame element equations. To validate the results of FlexFrame two examples are presented in Section 4. The results obtained by FlexFrame are compared with those reported in the literature. The three types of connections used in the study and equations describing their behavior are presented in Section 5. Results of the parametric study are included in Section 6.

2. MOMENT-ROTATION MODELS

The moment-rotation relationships of beam-to-column connections have been widely studied and there have been many mathematical models proposed to fit the moment-rotation curve of Figure 1. These models vary widely in their ease of implementation, applicability to experimental data, and complexity of mathematical formulation.

The first of these is the linear model which states that the ratio of the beam moment, M, to the connection rotation, θ_r, is constant, i.e.

$$M = K\theta_r \tag{1}$$

where K is the stiffness of the linear rotational spring connecting the beam and column. The imaginary case of a fully restrained connection capable of developing an infinite moment would have an infinite value of K. An imaginary pinned connection would have a value of $K = 0$. This model is simple and easy to implement, but in reality, no connection is linear throughout the entire M-θ_r curve.

The first attempt at a better approximation is a bi-linear model with the slope of the first line representing the initial connection stiffness, K_i, and the slope of the second line, K_p ($< K_i$), representing the stiffness after connection plasticity had occurred. K_p is equal to zero for the case of a connection that is perfectly plastic. This bi-linear model has been expanded to tri-linear, quad-linear, and higher poly-linear models.

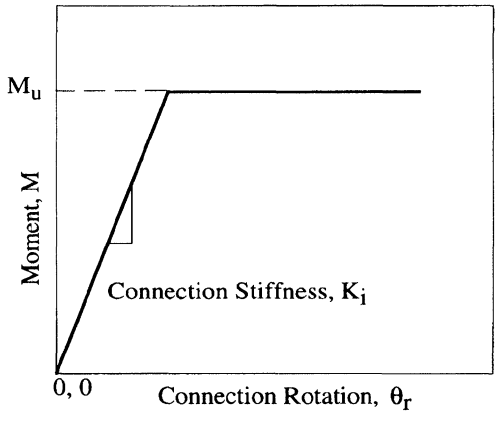

Fig. 2. Modeled connection behavior.

The next approximation is a polynomial expression of the form of equation 2.

$$\theta = \Sigma C_i (KM)^{\alpha i} \tag{2}$$

This model has the advantage of being smooth and easily differentiable; the constants, however, have very little physical meaning and the slope of the function can become zero or negative. Following these are the Richard-Abbott, cubic b-spline, Ramberg-Osgood, and the exponential formulas, each having relative success at matching experimental data but having the disadvantage of difficulty of implementation, or inapplicability to some types of connection data.[6]

While the later mathematical formulations generally have shown to be excellent at matching the moment-rotation curve, the bi-linear model has the advantage of being simple to understand and implement by practicing engineers and has been found to be capable of capturing the essence of the structure behavior.[7] Therefore, the bi-linear model has been chosen for the analyses presented in this paper. The slope of the first line being equal to the initial stiffness K_i, and (with $K_p = 0$) the value of the second line equal to the ultimate connection moment M_u.

3. PLANE FRAME EQUATIONS INCLUDING CONNECTION FLEXIBILITY AND PLASTICITY

Some of the key equations of frame analysis are included in this section. For a detailed coverage of traditional frame analysis the reader is directed to a book on structural or finite element analysis.[8] The stiffness matrix for a frame element, shown in Figure 3, with rigid connections is given by the following equation.

$$k = \begin{bmatrix} \frac{EA}{L} & 0 & 0 & -\frac{EA}{L} & 0 & 0 \\ & \frac{12EI}{L^3} & \frac{6EI}{L^2} & 0 & -\frac{12EI}{L^3} & \frac{6EI}{L^2} \\ & & \frac{4EI}{L} & 0 & -\frac{6EI}{L^2} & \frac{2EI}{L} \\ & & & \frac{EA}{L} & 0 & 0 \\ & & & & \frac{12EI}{L^3} & -\frac{6EI}{L^2} \\ \text{S} & \text{y} & \text{m} & \text{m.} & & \frac{4EI}{L} \end{bmatrix} \tag{3}$$

where

L = element length
E = Young's modulus
I = moment of inertia and
A = area of cross section.

The fixed-end forces due to a uniformly distributed load of magnitude, q, are given by the following equation.

$$f=\left[0\ \frac{qL}{2}\ \frac{qL^2}{12}\ 0\ \frac{qL}{2}\ -\frac{qL^2}{12}\right]^T \tag{4}$$

The superscript T indicates transpose of the vector.

P-Delta Effect

The application of gravity loads to a structure which is also subjected to lateral loading will cause the lateral drift of the structure to increase. This is described as the *P*-Delta effect, where *P* represents the axial load of a member (column) and Delta represents the story drift. The LRFD requires that this effect be taken into account for a PR type analysis. In the mathematical formulation, first the original element stiffness matrix, k, is computed and used to solve for the joint displacements and member forces, including the axial force, P, in each member. The member stiffness, k, is then adjusted by subtracting the so-called *geometric* stiffness matrix, k_g.[9]

$$k_g = P\begin{bmatrix} 0 & 0 & 0 & 0 & 0 & 0 \\ & -\frac{6}{5L} & -\frac{1}{10} & 0 & \frac{6}{5L} & -\frac{1}{10} \\ & & -\frac{2L}{15} & 0 & \frac{1}{10} & \frac{L}{30} \\ & & & 0 & 0 & 0 \\ & & & & -\frac{6}{5L} & \frac{1}{10} \\ \text{S} & \text{y} & \text{m} & \text{m.} & & -\frac{2L}{15} \end{bmatrix} \tag{5}$$

The modified k matrix is then used again to solve for the displacements and forces. This process is repeated until the lateral drift converges, usually within 2 or 3 iterations. The details of the solution algorithm can be found in Reference.[9]

Connection Flexibility

The effect of connection flexibility of the beam-to-column joint is modeled by attaching rotational springs of moduli k_L and k_R to the member ends as shown in Figure 4.

The element stiffness matrix is obtained as follows.[10]

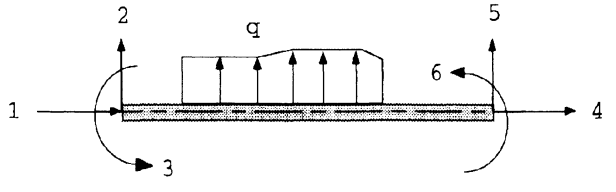

Fig. 3. A rigid frame element.

$$K=\alpha\begin{bmatrix} \frac{EA}{\alpha L} & 0 & 0 & -\frac{EA}{\alpha L} \\ & \frac{L}{EI}+\frac{1}{k_L}+\frac{1}{k_R} & \frac{L^2}{2EI}+\frac{L}{k_R} & 0 \\ & & \frac{L^3}{3EI}+\frac{L^2}{k_R} & 0 \\ & & & \frac{EA}{\alpha L} \\ \text{S} & \text{y} & \text{m} & \text{m.} \end{bmatrix}$$

$$\begin{bmatrix} 0 & 0 \\ -\frac{L}{EI}-\frac{1}{k_L}-\frac{1}{k_R} & \frac{L^2}{2EI}+\frac{L}{k_L} \\ -\frac{L^2}{2EI}-\frac{L}{k_R} & \frac{L^3}{6EI} \\ 0 & 0 \\ \frac{L}{EI}+\frac{1}{k_L}+\frac{1}{k_R} & -\frac{L^2}{2EI}-\frac{L}{k_L} \\ & \frac{L^3}{3EI}+\frac{L^2}{k_L} \end{bmatrix} \tag{6}$$

where

$$\alpha=\frac{1}{L^2\left[\left(\frac{L}{3EI}+\frac{1}{k_L}\right)\left(\frac{L}{EI}+\frac{1}{k_L}+\frac{1}{k_R}\right)-\left(\frac{L}{2EI}+\frac{1}{k_L}\right)^2\right]} \tag{7}$$

The fixed end forces due to uniformly distributed loads are

$$f=[0\,f_2\,f_3\,0\,f_5\,f_6]^T$$

where

$$f_2=\frac{qL}{2}\left[\frac{\left(\frac{L}{2EI}+\frac{1}{k_R}\right)\left(\frac{L}{3EI}+\frac{1}{k_R}\right)-\left(\frac{L}{4EI}+\frac{1}{k_R}\right)\left(\frac{L}{EI}+\frac{1}{k_L}+\frac{1}{k_R}\right)}{\left(\frac{L}{2EI}+\frac{1}{k_R}\right)^2-\left(\frac{L}{3EI}+\frac{1}{k_R}\right)\left(\frac{L}{EI}+\frac{1}{k_L}+\frac{1}{k_R}\right)}\right] \tag{8}$$

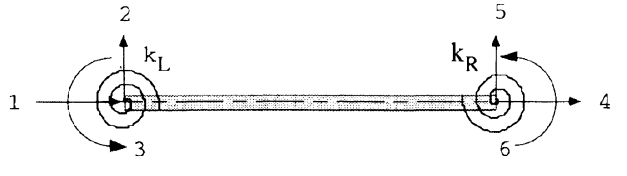

Fig. 4. Flexibly connected frame element showing rotational springs.

$$f_3 = \frac{qL^2}{2}\left[\frac{\left(\frac{L}{3EI}+\frac{1}{k_R}\right)^2 - \left(\frac{L}{4EI}+\frac{1}{k_R}\right)\left(\frac{L}{2EI}+\frac{1}{k_R}\right)}{\left(\frac{L}{2EI}+\frac{1}{k_R}\right)^2 - \left(\frac{L}{3EI}+\frac{1}{k_R}\right)\left(\frac{L}{EI}+\frac{1}{k_L}+\frac{1}{k_R}\right)}\right] \quad (9)$$

$$f_5 = \frac{qL}{2}\left[\frac{\left(\frac{L}{2EI}+\frac{1}{k_L}\right)\left(\frac{L}{3EI}+\frac{1}{k_L}\right) - \left(\frac{L}{4EI}+\frac{1}{k_L}\right)\left(\frac{L}{EI}+\frac{1}{k_L}+\frac{1}{k_R}\right)}{\left(\frac{L}{2EI}+\frac{1}{k_L}\right)^2 - \left(\frac{L}{3EI}+\frac{1}{k_L}\right)\left(\frac{L}{EI}+\frac{1}{k_L}+\frac{1}{k_R}\right)}\right] \quad (10)$$

$$f_6 = \frac{qL^2}{2}\left[\frac{\left(\frac{L}{3EI}+\frac{1}{k_L}\right)^2 - \left(\frac{L}{4EI}+\frac{1}{k_L}\right)\left(\frac{L}{2EI}+\frac{1}{k_L}\right)}{\left(\frac{L}{2EI}+\frac{1}{k_L}\right)^2 - \left(\frac{L}{3EI}+\frac{1}{k_L}\right)\left(\frac{L}{EI}+\frac{1}{k_L}+\frac{1}{k_R}\right)}\right] \quad (11)$$

Note that Equations 8-11 reduce to Equation 4 when the spring stiffnesses beccome very large.

Connection Plasticity

The connection plasticity is accounted for by applying the load in steps. First, the total load is applied which produces the joint displacements, d_{jo}, and member forces, m_{fo} which correspond to the linear behavior of the frame without connection plasticity. For the joint i, the ratio of the connection ultimate capacity, M_{ui}, to the applied moment, M_{oi}, is defined as α_i.

$$\alpha_i = \frac{M_{ui}}{M_{oi}} \quad (12)$$

This ratio is computed for each connection and the maximum α_i for all connections is defined as α_{max}.

$$\alpha_{max} = \max(\alpha_1, \alpha_2, \ldots, \alpha_{2m}) \quad (13)$$

If α_{max} is less than 1, then there is no connection plasticity. If α_{max} is greater than 1, then the joint displacements d_{jo} and member forces m_{fo} are reduced by the factor α_{max} to produce the joint displacements, d_{ja}, and member forces, m_{fa}, corresponding to the values at the point of yielding of the critical connection. These joint displacements and member forces are then added to the total structure displacements and member forces. The remaining moment capacity, M_p, of each member is then reduced by the moment already developed in the member, and the remaining load is applied to the frame. This process is continued until all of the load has been applied. The P-Delta effects are taken into account during each load step.

This incremental loading to the yield of the critical connection and subsequent reduction of structure stiffness produces the behavior shown in Figure 5. The load factor is the fraction of the total structure load applied. As the load is applied, the frame sway increases until the moment at the weakest connection reaches L_1, which corresponds to a lateral sway of Δ_1. This critical connection then becomes unable to sustain additional load, and the structure stiffness is decreased. This continues until either the entire load is supported without any more connections reaching their ultimate moment or all of the connections yield and the frame becomes unstable. For the results presented in this paper it was assumed that the members themselves remained elastic throughout. The plasticity was limited to the beam-to-column joints.

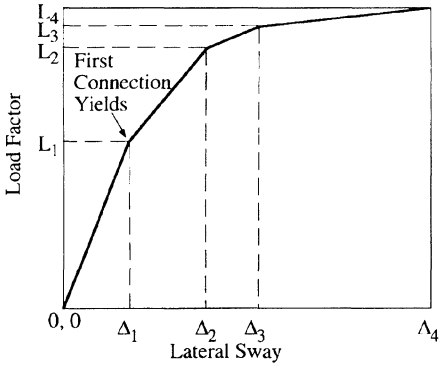

Fig. 5. Effect of connection plasticity on lateral sway.

4. FLEXFRAME VALIDATION

In order to verify the results of FlexFrame, two example frames shown in Figures 6 and 7 are selected from a recent paper by King and Chen.[11]

The frames are analyzed assuming rigid and flexible connections, with and without P-Delta effects. For all analyses E was assumed to be 29000 ksi. For flexible connections the following values for initial stiffness and ultimate moment were used.

K_i = 786,732 k-in/rad M_u = 1989

The loading was as follows.

For Example 1: P = 100 kips H = 10 kips
For Example 2: w = 0.15 k/in H = 7.0 kips

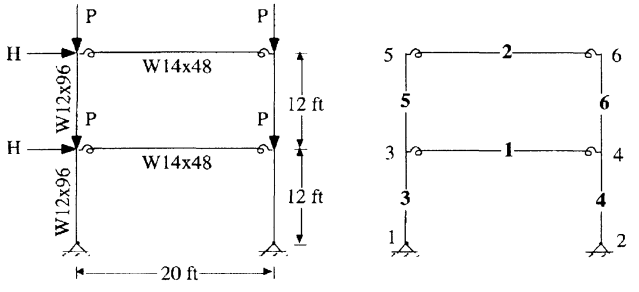

Fig. 6. Example frame 1.

Table 1a. Lateral Displacements (in.) for Example Frame 1					
	Rigid No *P*-Delta	Rigid connections with *P*-Delta		Flexible connections with *P*-Delta	
Node #	FlexFrame	FlexFrame	King & Chen	FlexFrame	King & Chen
3	1.011	1.168	1.16	1.477	2.02
5	1.509	1.731	1.82	2.292	3.26

Table 1b. Absolute Maximum Bending Moments (kip-in.) for Example Frame 1					
	Rigid No *P*-Delta	Rigid connections with *P*-Delta		Flexible connections with *P*-Delta	
Elem. #	FlexFrame	FlexFrame	King & Chen	FlexFrame	King & Chen
1	1450	1654	1649	1634	1560
2	711	795	794	902	1116
3	1443	1677	1670	1739	1837
4	1437	1669	1664	1731	1834
5	711	794	794	902	1116
6	711	795	794	902	1116

The analysis results are summarized in Tables 1 and 2.

It is clear from Tables 1 and 2 that for both examples the results of FlexFrame with rigid connections are almost identical to those reported by King & Chen. However for flexible connections the results are different. The lateral drift values produced by FlexFrame are lower than those reported. The differences are attributed to the way the connections are modeled. In reference[11] King and Chen have used a nonlinear moment rotation relationship given by the following equation.

$$\frac{dM}{d\theta_r} \equiv K_t = K_i\left[1 - \left(\frac{M}{M_u}\right)^c\right]$$

where

K_t = tangent stiffness
K_i = initial connection stiffness
M_u = ultimate bending moment capacity
M = connection moment
c = shape factor accounting for decay rate of K_i.

In the FlexFrame computer program a simple bi-linear model

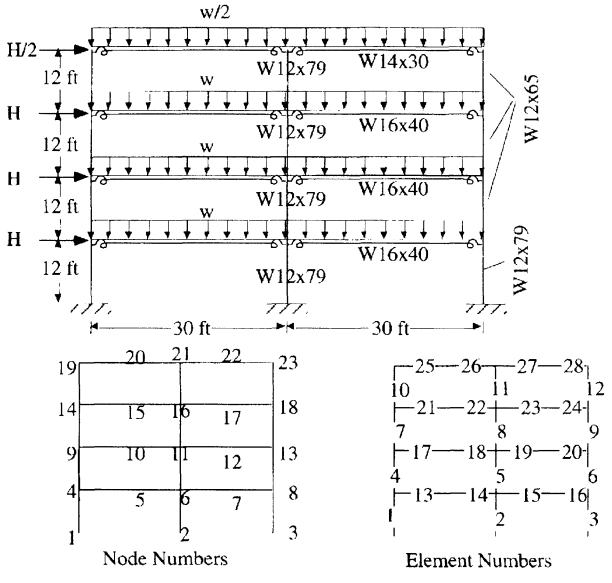

Fig. 7. Example frame 2.

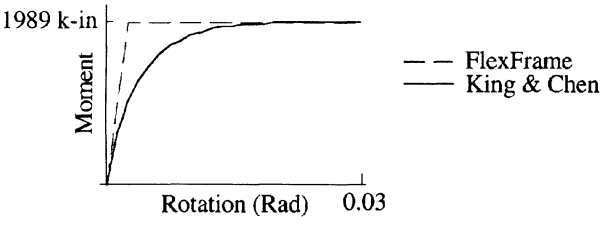

Fig. 8. Connection moment-rotation curves for the example frames.

Table 2a.
Lateral Displacements (in.) for Example Frame 2

Node #	Rigid connections with *P*-Delta		Flexible connections with *P*-Delta	
	FlexFrame	King & Chen	FlexFrame	King & Chen
4	0.269	0.27	0.304	0.4
9	0.663	0.66	0.771	1.07
14	0.941	0.94	1.116	1.61
19	1.109	1.11	1.328	1.95

is used to describe moment rotation characteristics of a flexible joint. Figure 8 compares the connection moment-rotation relationship used in FlexFrame and that used by King and Chen. Since the connection stiffness is assumed to remain constant at its initial value, the FlexFrame results are expected to give lower drift values than those given in reference.[11] This trend is clear in the results shown in Tables 1 and 2.

5. MODELING OF CONNECTIONS

The equations used to relate the connection geometry to the parameters K_i and M_u were derived by Kishi and Chen[5] using finite element analysis of the connection at both service load and failure. This analysis neglects the effect of shear and deformation of the column or beam.

Single and Double Web-angle Connections

The double web-angle connection used in this study is shown in Figure 9. Figure 10 shows the web-angle at failure and includes the geometric parameters used in the equations for K_i and M_u for the web-angle connections.

Initial Elastic Stiffness

$$K_i = n_w G \frac{t_a^3}{3} \frac{\alpha\cosh(\alpha\beta)}{\alpha\beta\cosh(\alpha\beta) - \sinh(\alpha\beta)} \qquad (14)$$

where

$\alpha = 4.2967$

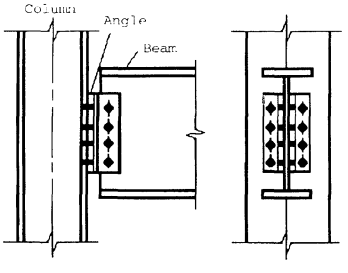

Fig. 9. Double web-angle connection.

Table 2b.
Absolute Maximum Bending Moments (kip-in.) for Example Frame 2

Elem. #	Rigid connections with *P*-Delta		Flexible connections with *P*-Delta	
	FlexFrame	King & Chen	FlexFrame	King & Chen
1	534	534	619	843
2	957	958	1016	1170
3	1202	1202	1254	1397
4	455	455	404	291
5	657	656	649	596
6	1102	1101	1064	1044
7	615	615	591	559
8	474	473	496	542
9	1029	1029	1005	996
10	704	702	687	705
11	200	200	225	313
12	820	818	812	846

$$\beta = \frac{g_1}{l_p}$$

$$g_1 = g_c - k_a - \frac{w}{2}$$

$n_w = 1$ for single web angles and = 2 for double web angles.

Ultimate Moment Capacity

$$M_u = n_w l_p^2 \frac{2V_{pu} + V_0}{6} \left(\frac{V_{pu}}{V_0}\right)^4 + \frac{g_y}{t}\frac{V_{pu}}{V_0} - 1 = 0 \qquad (15)$$

where

$$V_0 = \frac{s_y l_p t_a}{2}$$

$$g_y = \frac{l_p g_1}{l_p - c_u}$$

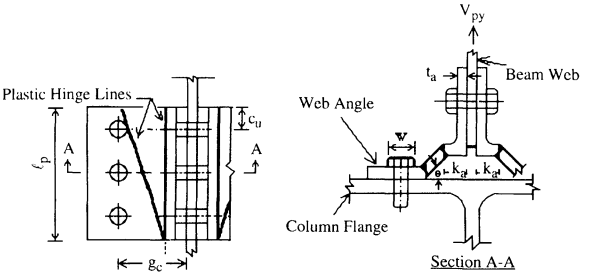

Fig. 10. Double-web-angle failure mechanism.

Table 3. Parameters Varied in Web-Angle Connection Study		
Parameter	Range (inches)	Nominal Value (inches)
g_c	1.5–2.5	2
k_a	0.625–1.0	0.875
l_p	5–13	7
t_a	0.25–0.6875	0.5

$$g_1 = g_c - k_a - \frac{w}{2}$$

The range of values used in the parametric study as well as the nominal values are listed in Table 3.

C_u and w were held constant at 2 inches and 1.125 inches respectively. 1.125 inches corresponds to a ¾-in. bolt diameter. All bolts were assumed to be A325.

Top and Seat-angle Connections

The top and seat-angle connection used in this study is shown in Figure 11. A close-up of the top-angle showing the fillet is presented in Figure 12. This figure also shows the top-angle at failure and includes the geometric parameters used in the equations for K_i and M_u for the top-angle connection.

Initial Elastic Stiffness

$$K_i = \frac{3EI_t d_1^2}{g_1^3\left(1 + \frac{0.78t_t^2}{g_1^2}\right)} \qquad (16)$$

where

$$I_t = \frac{l_t t_t^3}{12}$$

$$d_1 = d + \frac{t_s}{2} + \frac{t_t}{2}$$

$$g_1 = g_t - \frac{w}{2} - \frac{t_t}{2}$$

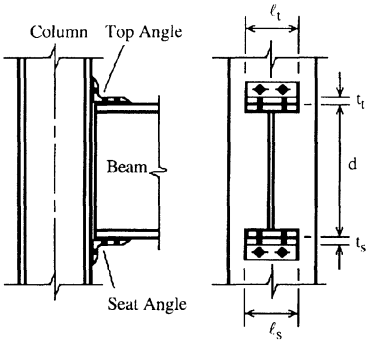

Fig. 11. Top and seat-angle connection.

Table 4. Parameters Varied in Top and Seat-Angle Connection Study		
Parameter	Range (inches)	Nominal Value (inches)
g_t	2.25–3.5	2.75
k_t	0.875–1.5	1.1875
l_s	4.0–9.0	3.5
l_t	4.0–9.0	3.5
t_s	0.4375–1.0	0.5
t_t	0.4375–1.0	0.5

Ultimate Moment Capacity

$$M_u = M_{Os} + M_p + V_p d_2 \qquad (17)$$

where

$$M_{Os} = \frac{s_y l_s t_s^2}{4}$$

$$M_p = \frac{V_p g_2}{2}$$

$$\left(\frac{V_P}{V_0}\right)^4 + \frac{g_2}{t_t}\frac{V_p}{V_0} - 1 = 0$$

$$d_2 = d + \frac{t_s}{2} + k_t$$

$$V_0 = \frac{s_y l_t t_t^2}{2}$$

$$g_2 = g_t - k_t - \frac{w}{2} - \frac{t_t}{2}$$

s_y = yield strength of steel

The range of values used in the parametric study as well as the nominal values are listed in Table 4.

For simplicity d and w were held constant at 23.92 inches and 1.125 inches respectively. 1.125 inches corresponds to a ¾-in. bolt diameter. All bolts are assumed to be A325.

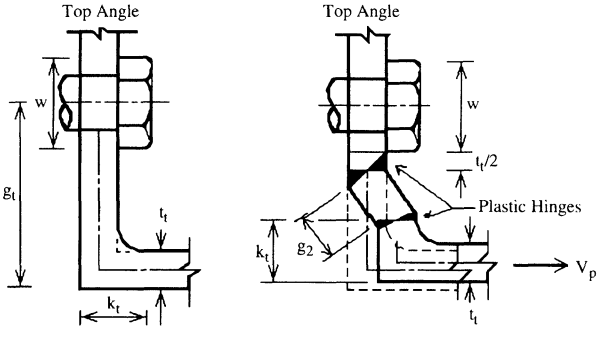

Fig. 12. Top-angle diagram showing fillet and mechanism of failure.

Table 5. Parameters Varied in Top and Seat with Double Web-Angle Connection Study					
Parameter	Range (in.)	Nominal Value (in.)	Parameter	Range (in.)	Nominal Value (in.)
g_c	2.5–7.5	3.5	l_p	3.0–13.0	9.0
g_t	2.5–4.5	3.5	l_s	4.0–9.0	7.0
k_a	0.5625–1.0625	0.75	l_t	4.0–9.0	7.0
k_t	0.75–1.375	1.0625	t_a	0.125–0.625	0.375
t_s	0.25–0.8125	0.5	t_t	0.25–0.8125	0.5

Top and Seat-angle with Web-angle Connections

The top and seat angle with double web-angle connection used in this study is shown in Figure 13. The figure shows the connection at failure and includes the relevant geometric parameters used in the equations for K_i and M_u for the top and seat angle with double web-angle connection.

Initial Elastic Stiffness

$$K_i = \frac{3EI_t d_1^2}{g_1(g_1^2 + 0.78t_t^2)} + \frac{6EI_a d_3^2}{g_3(g_3^2 + 0.78t_a^2)} \tag{17}$$

where

$$d_1 = d + \frac{t_t}{2} + \frac{t_s}{2}$$

$$I_t = \frac{l_t t_t^3}{12}$$

$$g_1 = g_c - k_a - \frac{w}{2}$$

$$d_3 = \frac{d}{2} + \frac{t_s}{2}$$

$$I_a = \frac{l_a^3 t_a}{12}$$

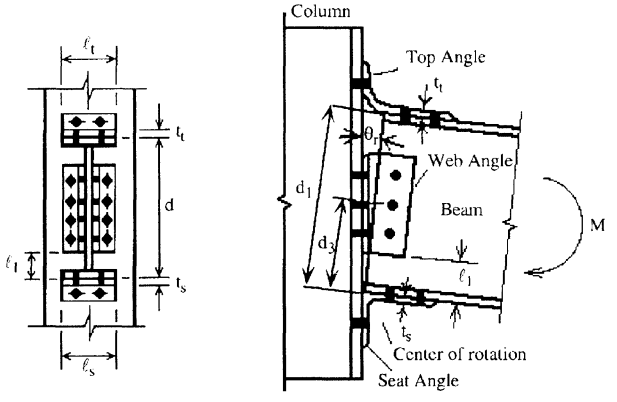

Fig. 13. Top and seat-angle with double web-angle connection.

$$g_3 = g_c - \frac{t_a}{2} - \frac{w}{2}$$

Ultimate Moment Capacity

$$M_u = M_{Os} + M_{pt} + V_{pt} d_2 + 2V_{pa} d_4 \tag{18}$$

where

$$M_{Os} = \frac{s_y l_s t_s^2}{4}$$

$$\left(\frac{V_{pt}}{V_{Ot}}\right)^4 + \frac{g_2}{t_t}\frac{V_{pt}}{V_{Ot}} - 1 = 0$$

$$V_{Ot} = \frac{s_y l_t t_t}{2}$$

$$M_{pt} = \frac{V_{pt} g_2}{2}$$

$$\left(\frac{V_{pu}}{V_{Oa}}\right)^4 + \frac{g_5}{t_a}\frac{V_{pu}}{V_{Oa}} - 1 = 0$$

$$V_{Oa} = \frac{s_y l_p t_a}{2}$$

$$V_{pa} = \frac{V_{pu} + V_{Oa}}{2} l_p$$

$$d_4 = \frac{2V_{pu} + V_{Oa}}{3(V_{pu} + V_{Oa})} l_p + l_1 + \frac{t_s}{2}$$

$$g_5 = \frac{g_1 l_p}{l_p - c_u}$$

$$g_1 = g_c - k_a - \frac{w}{2}$$

$$g_2 = g_t - k_t - \frac{w}{2} - \frac{t_t}{2}$$

$$d_2 = d + k_t + \frac{t_s}{2}$$

The range of values used in the parametric study as well as the nominal values are listed in Table 5.

It was also assumed that the web angle was centered vertically between the beam flanges, thus

$$l_1 = \frac{d - l_p}{2}$$

Table 6. Assumptions for Frame Analysis			
Dead Load	75 psf (6-in. slab)	Bay Width	20 feet
Live Load	100 psf	Frame Spacing	25 feet
Wind Load	25 psf (vertical area)	Acceptable Sway	H/400 = 840/400 = 2.1 inches
Story Height	14 feet	Beam Sections	W24×76
Column Sections	W14×90 (bottom 2 levels)	Column Sections	W14×61 (top 3 levels)

6. EFFECT OF CONNECTION PARAMETERS ON PLANE FRAME BEHAVIOR

A typical unbraced frame in an office building is used to study the effects of connection parameters on the behavior of plane frames. The frame consists of 3 bays and 5 stories and is shown in Figure 14. The loading data and other assumptions are presented in Table 6.

The moment developed at the connection was never allowed to exceed the plastic moment of the W24×76 beam section.

In the following sections different connection types are assumed for the frame. For each connection type, some of the design parameters are varied and their effect on the frame response is compared. The lateral sway of the frame is selected as the key frame response quantity for comparison purposes. The influence of connection parameters on the ultimate strength characteristics of the frame is not studied in this paper. Because of this choice all loading considered in the subsequent analyses is unfactored.

Before examining the effects of geometry it is useful to recognize the effect of connection flexibility and connection plasticity on the frame sway.

Connection Flexibility

The effect of connection stiffness on the frame lateral sway is shown in Figure 15. For very small values of connection stiffness the connection behaves like a simple connection which resists no moment. The entire lateral load is being resisted by the columns which are acting as full-height cantilever beams The values of sway which correspond to these "pinned" connections are governed by the rigidity of the columns. Notice that when P-Δ effects are included the frame sway is greatly magnified for small values of K_i ; for large stiffnesses, however, there appears to be almost no difference in frame sway, though the sway for the analysis including P-Δ effects remains greater than the analysis without P-Δ effects for all values of connection stiffness.

For very high values of connection stiffness the frame behaves like a rigidly connected frame with frame sway less than $H/400$.

Connection Plasticity

The effect of connection ultimate capacity on frame sway varies as a function of connection stiffness as shown in Figure 16. For low values of connection strength the curves approach the values given in Figure 15 for connections with very low connection stiffness (pinned connection). Notice that when P-Δ effects are included the frame sway is greatly magnified for small values of M_u ; for large connection strengths, however, there is no connection plasticity and the values of sway approach those of Figure 15. The sway for the analysis including P-Δ effects remains greater than the analysis without P-Δ effects for all values of connection strength.

Double Web-angle Connections

For the parametric study, only one parameter was varied at a time while the rest were kept at their nominal values.

The four parameters that were selected for the study of the double web-angle connection (as shown in Figure 10) are: g_c, the distance from the web-angle heel to the center of nearest bolt hole in the leg adjacent to the column face; k_a, the

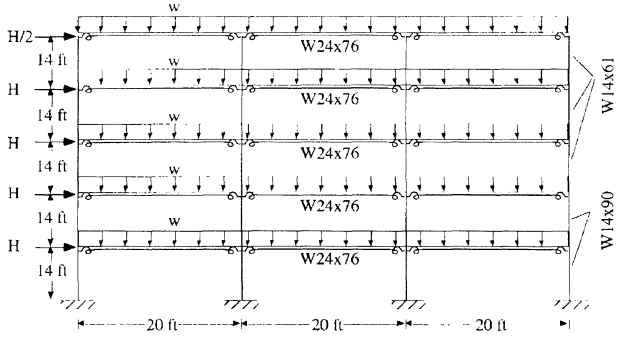

Fig. 14. 3-bay, 5-story frame.

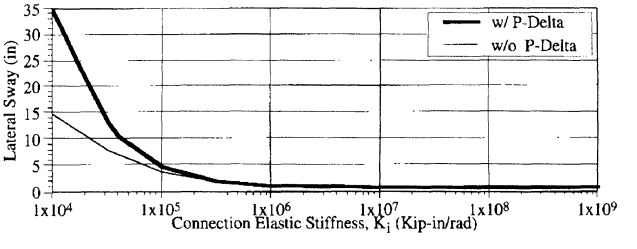

Fig. 15. Effect of connection stiffness on frame sway.

distance from web-angle heel to the toe of the fillet; l_p, the length of the web-angle and; t_a the thickness of the web-angle.

Figure 17 shows that the sway increases rapidly as g_c increases. This is mainly because the stiffness is reduced as the moment arm length increases, see Figure 10. There is connection yielding for g_c greater than 1.75 inches. Figure 18 shows that the sway decreases as k_a increases. This is because the failure is assumed to occur at the toe of the fillet, and a larger k_a reduces the leverage of the leg adjacent to the column flange. There was connection yield for all the cases shown in Figure 18. Figure 19 shows that the sway increases rapidly for l_p less than 8 inches. This increase is because the frame's connections are yielding for values of the web length under 8 inches. Figure 20 shows that the sway increases rapidly as t_a decreases. *P*-Delta effects cause the connections to yield when the web thickness is less than or equal to ½-in.

The large sway associated with double web-angle connections suggested that the sway for single web-angle connections would not be acceptable for this frame and loading arrangement. For instance, the nominal double web-angle configuration produced a lateral sway of 3.68 inches while the sway for the nominal single web-angle connection was 17.55 inches. Because of this, single web-angle connections were not investigated.

Top and Seat-angle Connections

The six parameters that were selected for the study of top and seat angle connection (as shown in Figure 11) are: g_t, the distance from the top-angle heel to the center of nearest bolt hole in the leg adjacent to the column face; k_t, the distance from top-angle heel to the toe of the fillet of the leg adjacent to the column face; l_s, the length of the seat-angle; l_t, the length of the top-angle; t_s, the thickness of the seat-angle, and t_t, the thickness of the top-angle.

Figure 21 shows an increase in sway as the value of g_t increases. Similar to the effect of g_c in the web-angle analysis, this is mainly because the stiffness is reduced as the moment arm length increases, as shown in Figure 12. However, the increase is not as rapid and the curve doesn't show a transition. This is because the connections have yielded. Figure 22 shows that the sway decreases as k_t increases. This is very similar to the aforementioned web-angle connection behavior except that this curve shows a flattening trend for lower values of the fillet width. There was connection yield for all the cases shown. Figure 23 shows a very small change in sway associated with the change in length of the seat angle. This is

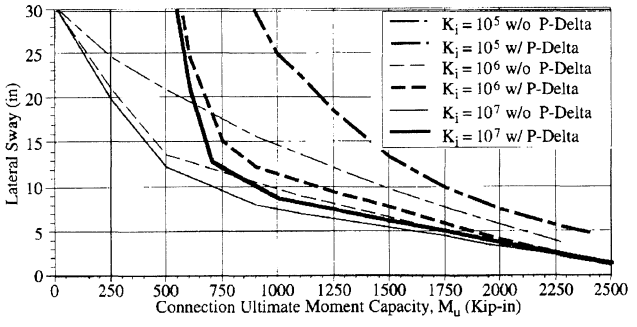

Fig. 16. Effect of connection strength on frame sway.

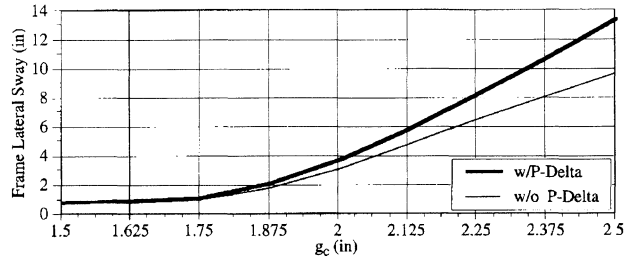

Fig. 17. Lateral sway vs. distance from web-angle heel to center of nearest bolt hole in the leg adjacent to column face (double web-angle connections).

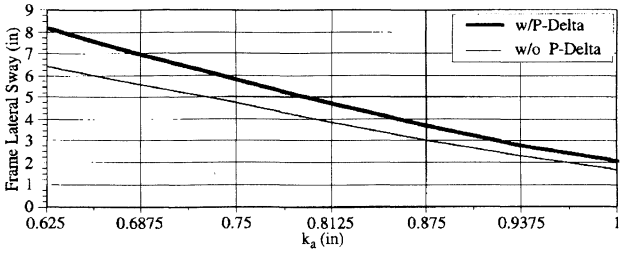

Fig. 18. Lateral sway vs. distance from web-angle heel to toe of fillet in the leg adjacent to column face (double web-angle connections).

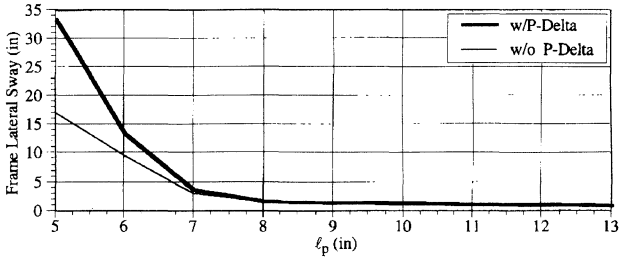

Fig. 19. Lateral sway vs. length of web-angle (double web-angle connections).

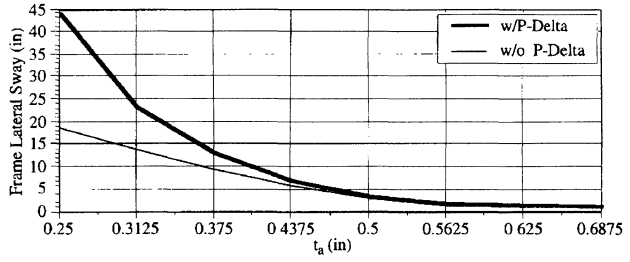

Fig. 20. Lateral sway vs. thickness of web-angle (double web-angle connections).

because the connections have yielded for all the cases shown and the failure mechanism is governed by the behavior of the top angle. The effect of top angle length on lateral sway is shown in Figure 24. There is an almost linear reduction in sway with an increase in the top angle length. However, it appears that the curve which includes *P*-Delta effects increases more rapidly for l_t less than 3 inches. The connections were yielding for all values of l_t shown.

Figure 25 shows that as the seat angle thickness is increased, the sway of the structure gradually decreases. This figure, together with the one showing the effect of the seat-angle length (Figure 23), emphasizes the fact that the seat-angle has little effect on the sway of the frame. However, the seat angle thickness is important in transferring shear to the column. The connections were yielding for all values of t_s shown.

For top and seat-angle connections the thickness of the top angle is the most important factor affecting the connection behavior as shown in Figure 26. This is because of the bending nature of the top-angle as previously illustrated by Figure 13. The connections were yielding for all values of t_t shown except for t_t = 1 inch.

Top and Seat with Web-angle Connections

The ten parameters that were selected for the study of the top and seat angle with double web-angle connection (as shown in Figure 13) are: g_c and g_t, the distance from the web- and top-angle heel to the center of nearest bolt hole in the leg adjacent to the column face, respectively; k_a and k_t, the distance from web and top-angle heel to the toe of the fillet in the leg adjacent to the column face, respectively; l_p, l_s, and l_t, the length of the web/seat/top-angle; t_p, t_s, and t_t, the thickness of the web, top, and seat-angle, respectively.

Figure 27 shows that the sway increases gradually as g_c increases. There was no connection yielding. Figure 28 shows that the web-angle thickness has very little effect on the frame sway for t_a = 3/16-in. or greater. However, when t_a = 1/8-in. the connections yield and the sway increases rapidly even though it is still within acceptable limits. It may appear from Figure 29 that the thickness of the top angle has no apparent effect on frame sway. However, since the connection is very stiff and strong, the effects are not as noticeable. For the range of parameters shown in Figure 29 the stiffness increases from 98.9 to 103.8 percent of the nominal stiffness and the strength increases from 94.8 to 112 percent of nominal. Figure 30 shows behavior similar to the previous graphs except for a dramatic increase in sway when the length of the web-angle decreases below 5 inches. To illustrate the behavior of the structure at l_p = 3 and l_p = 4 the load-sway plot is shown in Figure 31. It also shows that once the plastic limit of the first critical connection is reached, the connections fail in rapid succession. This is because there is redistribution of moment in a frame with uniform connection types. This figure also emphasizes the increased contribution of sway from *P*-Delta at the upper load levels.

In their respective parameter ranges (Table 5) the values of g_t, k_a, k_t, l_s, l_t, and t_s had only a very small (< 0.01 inch) effect on the sway, similar to Figure 29. The value of sway for these parameters was approximately 0.782 inches without *P*-Delta and 0.815 inches when *P*-Delta effects were included.

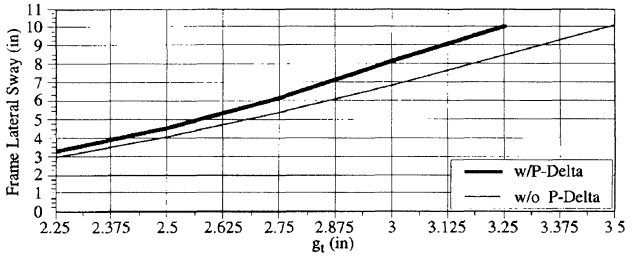

Fig. 21. Lateral sway vs. distance from top-angle heel to center of nearest bolt holes in leg adjacent to column face (top and seat-angle connections).

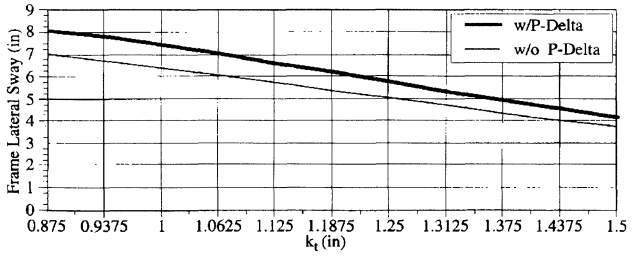

Fig. 22. Lateral sway vs. distance from top-angle heel to toe of fillet in leg adjacent to column face (top and seat-angle connections).

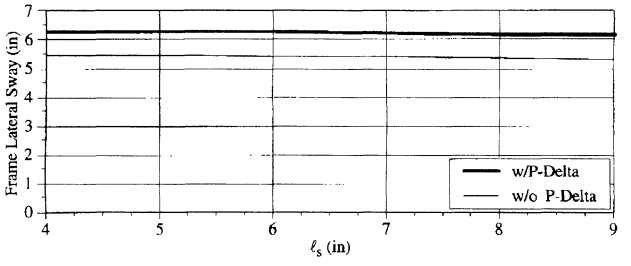

Fig. 23. Lateral sway vs. seat-angle length (top and seat-angle connections).

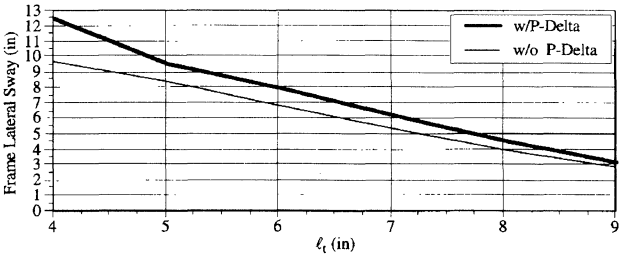

Fig. 24. Lateral sway vs. top-angle length (top and seat-angle connections).

7. CONCLUSIONS

The main objective of the detailed parametric study presented in the paper is to develop a feel for the effects of different connection parameters on the behavior of unbraced frames. Before presenting some general conclusions it should be emphasized that the quantitative results apply strictly only to the frame studied and are based on an acceptable sway criteria of H / 400. For other frames the graphs presented in the paper can only be used in a qualitative sense to guess at the general trends.

From the analyses presented it appears as if the double connections are not acceptable except only for extremely heavy connections. The single web-connections would not be feasible. The top and seat-angle connections would only be acceptable with thick top angles. It should be noted that although some of the proposed connection geometries would be acceptable based on sway, they would not be geometrically feasible, such as g_c = 1.5 inches. These were included in the study for comparison purposes. The top and seat angle with double web angle connections are satisfactory for almost all configurations investigated. For the double web-angle connection, the most important parameter is the thickness of the web angle, t_a, and the least is the distance from the web-angle heel to the toe of the fillet, k_a. The web-angle length, l_p, has only a limited effect on sway for when the connections remain elastic. For the top and seat-angle connection, the first and second most important parameters are the top-angle thickness, t_t, and length, l_t, respectively, and the least important parameter is the seat-angle length, l_s. These results support the other authors conclusions[12] that the top and seat-angle connection can be assumed to be a rigid connection if the top angle is stiffened sufficiently. For the top and seat with double web-angle connection, almost any configuration will be satisfactory to support this frame's lateral loading. The web-angle's contribution to stiffness is much greater than that of the flange angles. If the web-angle length, l_p, or thickness, t_a, are severely reduced this will reduce the connection stiffness which will lower the connection strength.

It should be noted that all of the sway investigations were done using unfactored loads. The effects of column flange and panel zone deformation as well as beam shear were neglected.

It is recommended that further computer implementations include the more complex models of connection behavior. Adding the post plastic linear stiffness K_p to form a tri-linear model would be a relatively easy way to improve the model. The tri-linear model would be much less time consuming to run on a personal computer than the advanced models such as the cubic B-spline. Future work should also include models that allow for unloading so that they can be used in dynamic analysis. It is further recommended that more frames of different height and length be used, and with different combinations of lateral load, to determine the acceptability of using PR construction for tall buildings. Optimization of column and girder sections could also be done to reduce member and connection costs. This optimization could explore the feasibility of using flexible connections on frames with partial bracing or shear walls. Finally, the effect of composite construction on connection flexibility and strength should be explored.

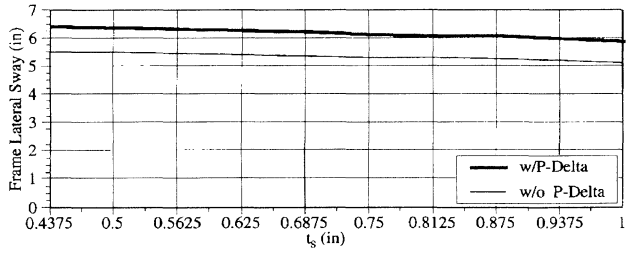

Fig. 25. Lateral sway vs. seat-angle thickness (top and seat-angle connections).

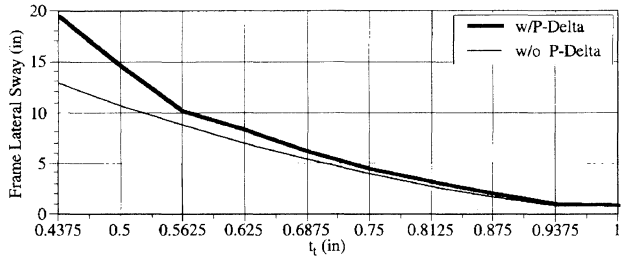

Fig. 26. Lateral sway vs. top-angle thickness (top and seat-angle connections).

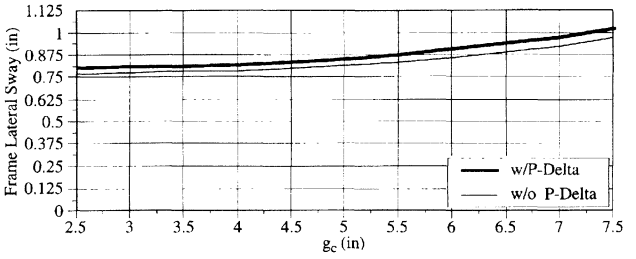

Fig. 27. Lateral sway vs. distance from web-angle heel to the center of nearest bolt holes in leg adjacent to column face (top and seat with web-angle connections).

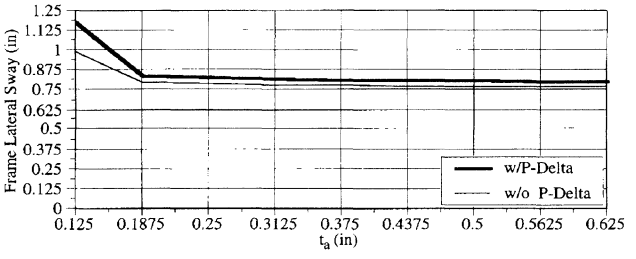

Fig. 28. Lateral sway vs. web-angle thickness (top and seat with web-angle connections).

REFERENCES

1. Azizinamini, A., *Monotonic Response of Semi-Rigid Steel Beam to Column Connections*, University of South Carolina, Columbia, SC, 1982.
2. *Load and Resistance Factor Design.* 1st edition, AISC, Chicago, IL, 1986.
3. Kishi, N. and Chen, W. F., *Data Base of Steel Beam-to-Column Connections (CE-STR-86-26)*, School of Civil Engineering, Purdue University, West Lafayette, IN, 1986.
4. Hingtgen, James D., "Effect of Connection Stiffness and Connection Plasticity on the Behavior of Unbraced Steel Frames Including Second Order Effects, M.S." Thesis, Department of Civil & Environmental Engineering, University of Iowa, Iowa City, IA, 1993.
5. Kishi, N. and Chen, W. F., *Moment-Rotation Relations of Semi-Rigid Connections*, School of Civil Engineering, Purdue University, West Lafayette, IN, 1987.
6. Nethercot, D. A., *Utilisation of Experimentally Obtained Connection Data in Assessing the Performance of Steel Frames, Connection Flexibility and Steel Frames*, American Society of Civil Engineers, Detroit, MI, 1985.
7. Gerstle, Kurt H. and Ackroyd, Michael H., "Behavior and Design of Flexibly-Connected Building Frames," *Engineering Journal*, Vol. 27, No. 1, 1990, pp. 22–29.
8. Chandrupatla, T. R. and Belegundu, A. D., *Introduction to Finite Elements in Engineering.* Prentice-Hall, Inc, Englewood Cliffs, NJ, 1991.
9. Chen, W. F. and Lui, E. M., *Stability Design of Steel Frames*, CRC Press, Boca Raton, FL, 1991.
10. Goble, G. G., *A Study of the Behavior of Building Frames with Semi-Rigid Joints*, AISC and The Ohio Steel Fabricators Association, Case Institute of Technology, 1963.
11. King, Won-Sun and Chen, W. F., "LRFD Analysis for Semi-rigid Frame Design," *Engineering Journal*, Vol.30, No. 4, 1993, pp. 130–140.
12. Leon, Roberto T., Ammerman, Douglas J., Lin, Jihshya, and McCauley, Robert D., "Semi-rigid Composite Steel Frames," *Engineering Journal*, Vol. 24, No. 4, 1987, pp. 147–155.

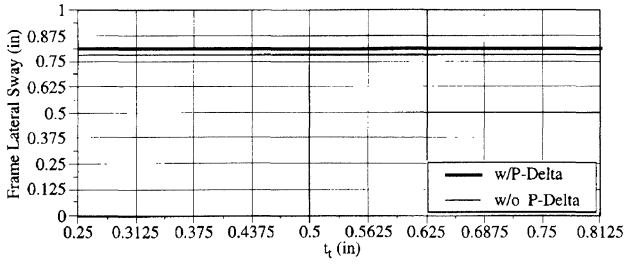

Fig. 29. Lateral sway vs. top-angle thickness (top and seat with web-angle connections).

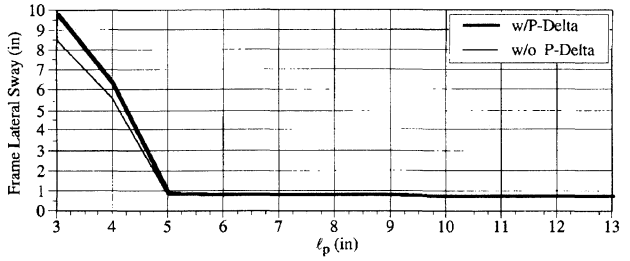

Fig. 30. Lateral sway vs. web-angle length (top and seat with web-angle connections).

LIST OF SYMBOLS

c_u distance from top of web angle to center of the nearest bolt hole
d depth of beam
g_c distance from the heel of the web angle to center of bolt holes in the leg adjacent to the column face
g_t distance from the heel of the top angle to center of bolt holes in the leg adjacent to the column face
k_a distance from the heel of the web angle to the toe of the fillet in the leg adjacent to the column face
k_t distance from the heel of the top angle to the toe of the fillet in the leg adjacent to the column face
l_1 distance from the bottom of the web angle to the bottom of the beam
l_p length of the web angle
l_s length of the seat angle
l_t length of the top angle
n_w number of web angles (= 1 for single web angles, = 2 for double web angles)
s_y yield strength of steel (= 36 ksi for structural steel)
t_a thickness of the web angle
t_s thickness of the seat angle
t_t thickness of the top angle
w width of the bolt head (or fasteners nut) across flats
E modulus of elasticity (= 29000 ksi for structural steel)
G shear modulus (= 11200 ksi for structural steel)
K_i elastic initial stiffness of connection
M_u ultimate moment capacity of connection

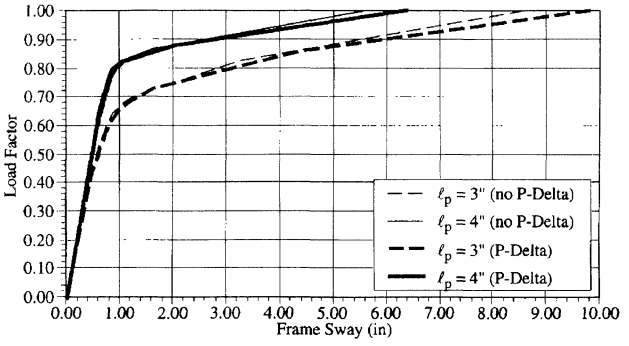

Fig. 31. Effect of web-angle length l_p, on frame sway and connection plasticity (top and seat with web-angle connections).